

BINARIZED SPIKING NEURAL NETWORK OPTIMIZED WITH GIZA PYRAMIDS CONSTRUCTION OPTIMIZATION ALGORITHM FOSTERED MELANOMA CLASSIFICATION FROM DERMOSCOPIC IMAGES

NALLANTI VENKATESWARARAO

Adikavi Nannaya University, Rajamahendravaram, Andhra Pradesh, India.
Email: nallanti2@gmail.com

Dr. PALLIPAMU VENKATESWARA RAO

Adikavi Nannaya University, Rajamahendravaram, Andhra Pradesh, India.
Email: pvr.cse@aknu.edu.in

Abstract

Melanoma is the major cause for death worldwide also called malignant skin cancer. Early diagnosis of melanoma by dermatoscopy particularly improves survival. However, exact detection of melanoma is very difficult for following reasons. Low contrast among lesions and skin, visually similar among melanoma and non-melanoma lesions, etc. Reliable, automated diagnosis of skin tumors would therefore greatly help improve accuracy and efficacy of pathologists. Here, Binarized Spiking Neural Network optimized with Giza Pyramids Construction Optimization Algorithm for automatic Melanoma Classification (BSNN-GPCOA-AMC-DI) from dermoscopic images is proposed. Primarily, the input Skin dermoscopic images are engaged from the dataset of Skin Lesion Images for Melanoma Classification. Then, the input Skin dermoscopic images is per-processed using Structural interval gradient filtering for removing noise and increase the quality of Skin dermoscopic images. Next, these pre-processed images are given to adaptive density-based spatial clustering for segmenting ROI region. The segmented ROI region is given into Ternary pattern and discrete wavelet transform for extracting Radiomic features such as Grayscale statistic features (standard deviation, mean, kurtosis, and skewness) and Haralick Texture features (contrast, energy, entropy, homogeneity, and inverse different moments). The extracted features are given into the Binarized Spiking Neural Networks which classifies the skin cancers such as Melanoma, nevus, Basal cell carcinoma, Actinic Keratosis, Pigmented Benign Keratosis, Dermatofibroma, Vascular lesion, Squamous cell carcinoma and seborrheic keratosis. In general, Binarized Spiking Neural Networks does not express any adaption of optimization strategies for determining the optimal parameters to assure accurate classification of skin cancer. Hence, Giza Pyramids Construction Optimization Algorithms proposed in this work to optimize the Binarized Spiking Neural Networks classifier, which precisely classifies the skin cancer. The proposed BSNN-GPCOA-AMC-DI method is implemented in MATLAB and the effectiveness is assessed with several performance metrics, like accuracy, precision, F score, sensitivity, specificity, ROC, computational time. Efficiency of proposed method BSNN - GPCOA-AMC-DI approach attains 10.12%, 22.33% high accuracy and 10.09%, 13.65% high precision is likened to the existing methods, such as Skin cancer classification of Convolutional Neural Network with optimized squeeze Net by Bald Eagle Search optimization (SCC - CNN - Squeeze Net - BES) and Skin cancer detection of Convolutional Neural Network using Gray Wolf Optimization (SCD - CNN - GWO) respectively.

Keywords: Melanoma classification, Binarized Spiking Neural Network, Giza Pyramids Construction Optimization Algorithm, Skin Lesion Images, Structural interval gradient filtering, Ternary pattern and discrete wavelet transform

1. INTRODUCTION

Melanoma is deadly skin cancer kills many people worldwide each year [1]. The main target areas are the parts of the human body that remain exposed to the sun, such as the face, arms, legs, and neck. Unfortunately, melanoma also has the highest mortality rate [2]. The main cause of melanoma is an abnormal increase in skin pigment produced by the body's cells. The melanoma moles that form change in figure, color like pink, red, black, and brown, based on seriousness of disease [3]. Melanoma is main reason of death around world and also called malignant skin cancer. Visual inspection of infected lesions allows detection of melanoma at an early stage [4-5]. A visual examination by a dermatologist is usual medical process to diagnose melanoma. Although, some problem in detecting melanoma. These difficulties include individual lesion morphology, lighting of clinical consulting area, patient skin tone, and expert experience in detecting melanoma. Detecting was subjective and challenge to repeat. Accurate medical detection is somewhat disappointment. To overcome the problem, we have to suggest some solutions to solve this problem.

In 2021, Sayed, et.al., [6] has suggested a melanoma prediction model utilizing optimized Squeeze Net by bald eagle search optimization. . It provides high accuracy with low precision. In 2021, Mohakud, et.al., [7] has presented a grey wolf optimization based hyper-parameter optimized Convolutional Neural Network classifier to detect skin cancer. It provides high precision rate with low accuracy. In 2020, Kumar, et.al., [8] has suggested DE-ANN inspired skin cancer diagnosis approach using fuzzy c-means clustering. It provides high accuracy with low specificity. In 2021, Balaji, et.al., [9] has presented examination of type of Neural Network for automated skin cancer categorization with firefly optimization. It provides high F score with low accuracy. Existing model do not give required accuracy for classifying Skin cancer and improves calculation time [6-9].

Major contribution to this work summarized here. Binarized A melanoma classification model is proposed with the help of Spiking Neural Network (BSNN). It is a Deep Model with conversion because of less parameters & accuracy. The diagnostic issues with Structural interval gradient filtering (SIGF) is utilized for removing noise and increase the quality of Skin Dermoscopic images. Performance of BSNN model progressed by implementing hyper parameter optimization with Giza Pyramids Construction Optimization Algorithm (GPCOA). Accuracy measures of melanoma classification method, with total accuracy of 98.37%, were improved when comparing to state-of-the-art methods utilizing similar data. Balance of this manuscript arranged as: proposed approach described in segment 2, outcomes and discussion is demonstrated in segment 3, conclusion is presented in segment 4.

2. PROPOSED METHODOLOGY

In this section, skin cancer classification with Binarized Spiking Neural Networks optimized with Giza Pyramids Construction Optimization Algorithm (BSNN - GPCOA-AMC-DI) is discussed. The block diagram of the proposed BSNN - GPCOA-AMC-DI skin

cancer classification is represented in Figure 1. It contains four stages, like acquisition of information, per-processing, Segmentation, extraction of feature, selection of feature and skin cancer categorization. Thus, detailed description about each stage is given below,

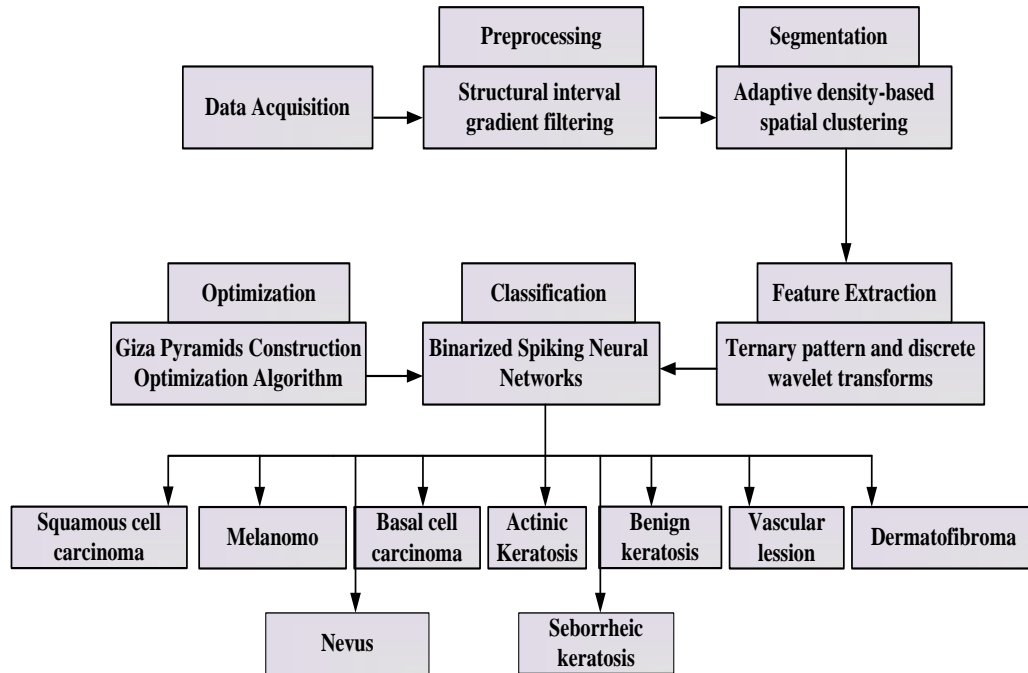


Figure 1: Block diagram of BSNN-GPCOA-AMC-DI methodology

2.1 Data Acquisition

In this step, the skin lesion image is taken from ISIC dataset to classify the skin cancer disease [15]. The dataset consist of 33,216 images from 2000 patients.

2.2 Pre-processing using Structural interval gradient filtering

In this step, Structural interval gradient filtering [10] performs the data pre-processing, which is utilized for removing noise and increase the quality of Skin dermoscopic images. Initially, Gaussian smoothing filtering is utilized for generating guided image g_{image} and it is represented in equation (1),

$$g_{image} = input_{skinlesionimage} * Gaussiansmoothingfilter \quad (1)$$

The interval gradient algorithm separated image to structure and texture. The textural portion contains bright patterns and flashy elements, while the structural portion contains protruding edges. The procedure of transforming a two-dimensional image to 1D signal by filtering of interval gradient. Then the output per-processing image are obtained and is represented in equation (2)

$$preprocessed\ outputimage = u * g_{image} + v(2) \quad (2)$$

Where u and v are linear coefficients. Equations (1) and (2) It preserves information in areas of high conflict and smooth out background non-dominant structures. Foreground detail may also be suppressed. The combination of structure preservation and spacing gradients effectively preserved foreground image and suppressant repeating texture design and structural details in background. The suggested filter forms better results to all type of other than hidden image and is expressed in equations (3) and (4).

$$H_{structurepreserving} = (H_{structure}) * E_{floodfill} \quad (3)$$

$$f(u,v) = [preprocessed\ output\ image - g_{image}]^2 + \mu * u^2 \quad (4)$$

Where μ are the linear coefficient. Finally, the per-processed skin lesion image using Structural interval gradient filtering is presented towards the segmentation phase.

2.3 Segmentation using Adaptive Density-Based Spatial Clustering

In this step, Adaptive Density-Based Spatial Clustering (Ada - DBSC) performs segmentation. This is used to segment the ROI region [11]. Ada - DBSC consists of four main modules, namely image block splitters. The image block splitter hierarchically allocates pixels into a series of blocks on idea of equal distribution. Local clustering, is local density-related clustering at every image block. GC is a process of joining local clusters to get clustering outcome. Image block used to merge 2 image blocks at GC. Ada - DBSC have top-down procedure that first applies an image block divider to divide the point to series of image blocks, and performs local cluster within every block. Obtaining the clustering result, Ada - DBSC done a global bottom-up clustering procedure in which image block merging plays major role.

The image block splitter provides splitting with equal distribution by scaling median information rate on every block, information entropy represented in equation (5),

$$S(Y) = \sum Q(y)T(y) = -\sum Q(y)\log_c Q(y) \quad (5)$$

Where, y is a random variable belongs to Y . $Q(y)$ is the occurrence probability of y . If image block splitter splits ROI in dimension, initial number of image blocks q represented in equation (6),

$$q = \left\lceil \sqrt{\frac{M}{f}} \right\rceil \quad (6)$$

Where f depicts points of expected average count at image block. Each image block find by lower and upper bound at standard coordinate scheme and is represented in equation (7) and (8),

$$h(u_j) = \min_j + \alpha_j u_j \quad (7)$$

$$h_u(u_j) = \min_j + (\alpha_j + 1)u_j \quad (8)$$

Where, u_j is the index of data block, $h(u_j)$ and $h_u(u_j)$ depicts lower and upper bound. To make image block splitter effectual, suggest a measure that block splitting at ROI region to some sub-blocks avoided and is represented in equation (9),

$$\alpha_s = \eta \cdot \varepsilon_{FATHER} + s + 1 \quad (9)$$

Where, ε_{FATHER} is the index of ROI region. Local cluster is density-related cluster procedure inside every discrete image block and is represented in equation (10),

$$e_1(c) = \min_j + \alpha p(c_i) \quad (10)$$

Where α bias of image block splitter, $e_1(c)$ denote the lower bound. Number of image points in block scope represented in equation (11),

$$Ep_{new} = \frac{E}{\beta} \times Ep_{new} \quad (11)$$

Ada - DBSC also done global clustering (GC) to get results of clustering. Since all clusters contained in blocks, GC is procedure of merging related local clusters and related image blocks. As a result of merging of blocks the image can segment the ROI region using Adaptive Density-Based Spatial Clustering and the segmented region can fed to feature extraction method.

2.4 Feature Extraction using Ternary pattern and discrete wavelet transforms

Here, particular features available under segmentation are cleared with Ternary pattern and discrete wavelet transforms (TP-DWT) [12]. From segmentation, it has significant characteristics for extracting Radiomic features such as Grayscale statistic features (standard deviation, mean, kurtosis, and skewness) and Haralick Texture features like contrast, energy, entropy, homogeneity, and inverse different moments. The progressed TP-DWT utilizes TP, DWT with statistical feature extraction. Major issue of TP is determining the threshold. Therefore, usage of standard deviations based on multi thresholds. The formula for multiple threshold determinations based on the standard deviation used can be expressed in Equation (12).

$$TH = sd(signal) * \frac{S}{10}, S = 1, 2, \dots, 10 \quad (12)$$

Where TH defines the threshold value. A statistical feature extraction function containing 20 statistical moments utilized to drive attributes from upper and lower ternary histograms. The features extracted from the TP-DWT method are shown below.

2.4.1 Grayscale statistic features

Grayscale statistic features like mean, standard deviation, skewness, and kurtosis are represented in equation (13-16),

$$mean = \frac{\sum_{j=1}^{256} TP-DWT}{256} \quad (13)$$

$$SD = \sqrt{\frac{1}{255} \sum_{j=1}^{255} \frac{TP-DWT-mean}{M}} \quad (14)$$

Where $TP-DWT-mean$ designates matrix and embodies image height and image width of TPDWT matrix.

$$Skewness = \sqrt{\frac{\sum_{j=1}^{255} TP-DWT^2}{256}} \quad (15)$$

$$kurtosis = \sum_{j=1}^{256} Q(TP-DWT) \log(Q(TP-DWT)) \quad (16)$$

2.4.2 Haralick Texture features

The Haralick Texture features represented in equation (17-21),

$$contrast = \sum_{j=1}^{256} \frac{j * TP-DWT-mean}{SD} \quad (17)$$

$$energy = \frac{\sum_{j=1}^{256} |(TP-DWT)_{j+1} - (TP-DWT)_j|}{256} \quad (18)$$

$$entropy = \frac{256 * 255}{254} \left(\frac{\frac{1}{256} \sum_{j=1}^{256} ((TP-DWT) - mean)^2}{\frac{1}{256} \sum_{j=1}^{256} ((TP-DWT) - mean)^3} \right)^{\frac{3}{2}} \quad (19)$$

$$homogeneity = \frac{255}{254 * 253} \left[257 - \frac{\left(\frac{1}{256} \sum_{j=1}^{256} ((TP-DWT) - mean)^4 \right)}{\left(\frac{1}{256} \sum_{j=1}^{256} ((TP-DWT) - mean)^2 \right)} - 3 \right] \quad (20)$$

$$inversedifferentmoments = \sqrt{\frac{\sum_{j=1}^{256} (TP-DWT)^2}{\frac{1}{256} \sum_{j=1}^{256} (TP-DWT)}} \quad (21)$$

Then these extracted features using Ternary pattern and discrete wavelet transforms are given into classification technique.

2.5 Skin cancer classification using Binarized Spiking Neural Networks

In this section, classifications of skin cancer using Binarized Spiking Neural Networks (BSNN) are discussed [13]. Input layer of suggested single-spike Binarized Supervised Spike Neural Network (BSNN) transforms input image to spike trains based on temporal coding to first spike. These spikes propagate through the network. The network does not allow hidden and output layer binary neurons to fire more than once. Every output neuron assigned to various section, and first resultant neuron to fire decides network's decision. Error for every resultant neuron is calculated by comparing the actual firing time to the target firing time. Next, we update the synaptic weights using a modified version of the SNN's back propagation algorithm. The training phase uses 2 sets of weights, real-valued weights W and corresponding binary weights. Input layer converting input image to bursts of peaks with a single-peak temporary encoding system known as intensity-to-latency conversion, expressed in equation (22).

$$s_j = \left\lfloor \frac{H_{\max} - H_{j(\max)}}{H_{\max}} \right\rfloor \quad (22)$$

Where, s_j is maximum classified region. By this way, input neurons of greater pixel intensities are short spike latencies. In this, utilized discretely and is represented in equation (23),

$$U_I^1(s) = U_I^1(s-1) + \beta^q \sum_j C_j T_{j-1}^u \quad (23)$$

Where, $U_I^1(s)$ is input spike pattern and binary synaptic weight. These measuring factors helps to stop enhancement of silent neurons is most probable to binary weights. Neuron fires once, 1st its membrane potential exceeds threshold, temporary error function of exact and goal firing, and is represented in equation (24),

$$f = [f_1, \dots, f_c] \quad f_i = (S_i^0 - s_i^0) / s_{\max} \quad (24)$$

Where s_i^0 and s_i^0 are original and goal firing times. To implement gradient descent approach, calculate loss function gradient with binary weights. Even so, gradient descent model creates little alterations of weights, can't done with binary scores. To solve issues, at learning stage, utilize group of real-valued weights and is represented in equation (25),

$$Q = \frac{1}{2} \|f\|^2 = \frac{1}{2} \sum_{i=1}^B f^2 \quad (25)$$

Major problems using single spike coding systems in SNNs is growth of died neurons at practice. While learning of particular stimulus, reduce neuron's weight to force it to the fire after, an opportunity weights differ in quantity that neuron can't get its threshold and for another input stimuli represented by equation (26),

$$\alpha_i^u = \sum_t \frac{\beta S}{\beta S_t^{u+1}} \frac{\beta S_t^{u+1}}{\beta Q_t^{u+1}} \frac{\beta Q_t^{u+1}}{\beta S_i^u} = \sum_t \alpha_i^{u+1} \beta^{u+1} + C_i^{u+1} \quad (26)$$

Where the scaling factor β is represented by $\beta = \beta^u - \chi \frac{\beta S}{\beta S_t}$. Before updating the weights normalize the gradients to keep off bursting and disappearing gradients. And, add L2-norm weight regularized term to loss function to stop over fitting and thus capture classified skin cancer images and is represented in equation (27),

$$\frac{\beta S}{\beta S_t} = \sum_i \frac{\beta S}{\beta S_t} \frac{\beta S_t}{\beta_i} = \sum_i \frac{\beta S}{\beta S_t} \frac{\beta S_t}{\beta Q_i^j} \frac{\beta Q_i^j}{\beta_i} = -\sum_i \alpha_i^u \sum_i C_i^u [S_t^u] \quad (27)$$

Where i iterate over the neuron layer. Finally, Binarized Spiking Neural Networks (BSNN) classifies the skin cancer disease as Normal, Melanoma, nevus, Basal cell carcinoma, Actinic Keratosis, Pigmented Benign keratosis, Dermato fibroma, Vascular lesion and Squamous cell carcinoma and Seborrheic keratosis.

In this work, Giza Pyramids Construction Optimization Algorithm (GPCOA) is exploited for optimizing the optimum parameters of Binarized Spiking Neural Networks (BSNN) classifier. Here, GPCOA is employed for tuning the weight and bias parameters of BSNN. Generally, some methods utilized for formation of constraint such as grid exploration, manual exploration and random exploration. Even so these finding transmit its uncommon weakness considering reiteration time and then, there is no subterfuge-assembled known enquiry. Therefore, GPCOA is utilized to overawe this problem.

2.5.1 Stepwise procedure of GPCOA

Here, stepwise procedure is depicted to obtain optimal scores of BSNN utilizing GPCOA [14]. Firstly, GPCOA makes equally distributed population to optimize optimal parameter of BSNN parameters. Optimal solution is promoted using GPCOA approach. Then, procedure of broad step shown here,

Step 1: Initialization

Initialize the population of workers as U . Initial part of block cost are familiar. Workers moving constantly to detect better place to control stone block optimizing weight parameter values of β from Binarized Spiking Neural Networks and is represented in equation (28),

$$f = \beta_s n u \cos \theta \quad (28)$$

Where n depicts the mass of the stone block, u is the gravity of the earth.

Step 2: Random generation

After initialization, input parameters randomly generated. Here, scores of better fitness selected according to explicit hyper parameter situation.

Step 3: Fitness Function Estimation

From initialized assessments, random output is produced. Fitness function appraised with the values of parameter optimization for optimizing weight parameter β of spike network and it is represented in equation (29),

$$fitness\ function = optimizing(\beta) \quad (29)$$

Step 4: Determine new position and new cost

After optimizing β amount of stone blocks displacement related to early region with the change to find a novel region of labor. For labor, friction not regarded. So, novel region of labour pushing stone block and represented in equation (30),

$$y = \frac{u_0^2}{2h\sin\theta} \quad (30)$$

After computing changes of stone block displacement and worker movement a novel position can received at result of 2 formulas. This novel position is new result and can be represented in equation (31),

$$q = (q + e) \times y \in_j \quad (31)$$

Step 5: Return new solution

At every repetition of approach, initial velocity regarded random number, because every time labour try to move stone block, implied force changes based on power used by worker and is represented in equation (32),

$$u_0 = rand(0,1) \quad (32)$$

Initial outcome will be replaced with created outcome. So to return novel outcome, and is represented in equation (34),

$$b_k = \begin{cases} \alpha_k & \text{if } rand(0,1) \\ \beta_k & \text{otherwise} \end{cases} \quad (33)$$

Step 6: Termination Condition

Here, weight parameter values of β from Binarized Spiking Neural Networks are optimized with GPCOA Algorithm, will repeat the step 3 until the halting criteria met. Then BSNN- GPCOA-AMC-DI classifies the skin cancer disease greater accuracy by lowering calculation time with error.

3. RESULT WITH DISCUSSION

The experimental result of suggested Binarized Spiking Neural Network optimized with Giza Pyramids Construction Optimization Algorithm fostered Melanoma Classification from Dermoscopic Images (BSNN- GPCOA-AMC-DI) method explained here. Simulations done in PC with Intel Core i5, 2.50 GHz CPU, 8GB RAM, Windows 7. Then,

suggested model simulated utilizing MATLAB under several performance metrics. Results of BSNN- GPCOA-AMC-DI method are analyzed with existing SCC-CNN-Squeeze Net-BES methods [6] and Skin cancer detection of Convolutional Neural Network using Gray Wolf Optimization (SCD-CNN-GWO) [7] respectively. The output of the proposed BSNN- GPCOA-AMC-DI shown in Figure 2


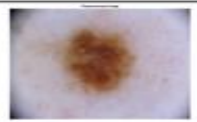

























Dataset	Input image	Preprocessing	Segmentation	Classification
Skin Lesion image				Nevus
				Basal cell carcinoma
				Actinic Keratosis
				Benign Keratosis
				Dermatofibroma
				Vascular lesion
				Squamous cell carcinoma
				Melanoma
				Seborrheic keratosis

Figure 2: Output images of skin cancer classification

3.1 Performance measures

This is particular task job classifier selection. To analyze performance, performance metrics are examined. True Negative, True Positive, False Negative and False Positive values are needed.

True Positive (TP): Accurate classification of diseased region from the normal region.

True Negative (TN): Inaccurate classification of diseased region into normal region.

False Positive (FP): Accurate classification of normal region from the diseased region.

False Negative (FN): Inaccurate classification of normal region into diseased region.

Accuracy is represented in equation (34),

$$Accuracy = \frac{TP}{TP + FP} \quad (34)$$

Precision is represented in equation (35),

$$Precision = \frac{TP}{TP + TN} \quad (35)$$

F score is represented in equation (36),

$$F\ score = \frac{TP}{\left(TP + \frac{1}{2}[TN + FP] \right)} \quad (36)$$

Sensitivity is represented in equation (37),

$$sensitivity = \frac{TN}{TN + FN} \quad (37)$$

Specificity is represented in equation (38),

$$specificity = \frac{TP}{FP + TP} \quad (38)$$

3.2 Performance Analysis

Table 1-4 depicts the simulation outcome of BSNN- GPCOA-AMC-DI method. Then, the proposed BSNN- GPCOA-AMC-DI comparing with existing SCC-CNN-Squeeze Net-BES and SCD-CNN-GWO models.

Table 1: Comparison of Accuracy Analysis

Techniques	Accuracy (%)								
	Melanoma	Basal cell carcinoma	Actinic Keratoses	Pigmented Benign keratoses	Dermatofibroma	Vascular lesion	Squamous cell carcinoma	Seborrheic keratosis	Nevus
SCC-CNN-Squeeze Net-BES	0.84	0.83	0.82	0.82	0.85	0.81	0.84	0.82	0.83
SCD-CNN-GWO	0.90	0.91	0.86	0.89	0.82	0.79	0.78	0.85	0.88
BSNN-GPCOA-AMC-DI(proposed)	98.95	98.87	98.99	98.88	98.75	99.08	98.09	98.69	98.96

Table1 demonstrates the Comparison of accuracy analysis. Here, the proposed BSNN-GPCOA-AMC-DI method provides 32.21%, 37.56% better accuracy for Melanoma classification; 25.45%, 45.89% better accuracy for Basal cell carcinoma classification; 23.21%, 32.56% better accuracy for Actinic Keratosis classification; 22.45%, 43.89% better accuracy for Pigmented Benign keratosis classification; 43.98%, 33.44% better accuracy for Dermatofibroma classification; 56.08%, 45.09% better accuracy for Vascular lesion classification; 32.09%, 45.67% better accuracy for Squamous cell carcinoma classification; 22.13%, 54.32% better accuracy for nevus classification; 11.22%, 18.76% better accuracy for seborrheic classification evaluated to the existing methods such as SCC-CNN-Squeeze Net-BES and SCD-CNN-GWO respectively.

Table 2: Comparison of Precision Analysis

Techniques	Precision (%)								
	Melanoma	Basal cell carcinoma	Actinic Keratosis	Pigmented Benign keratosis	Dermatofibroma	Vascular lesion	Squamous cell carcinoma	Seborrheic keratosis	Nevus
SCC-CNN-Squeeze Net-BES	0.79	0.85	0.82	0.85	0.80	0.87	0.89	0.86	0.79
SCD-CNN-GWO	0.87	0.87	0.81	0.84	0.81	0.88	0.84	0.82	0.77
BSNN-GPCOA-AMC-	0.99	0.98	1	0.99	1	0.98	1	1	0.99

DI(proposed)									
--------------	--	--	--	--	--	--	--	--	--

Table2 demonstrates the Comparison of precision analysis. Here, the proposed BSNN-GPCOA-AMC-DI method provides 42.21%, 47.56% higher precision for Melanoma classification; 55.45%, 65.89% higher precision for Basal cell carcinoma classification; 43.21%, 22.56% higher precision for Actinic Keratosis classification; 62.45%, 53.89% higher precision for Pigmented Benign keratosis classification; 53.98%, 63.44% higher precision for Dermatofibroma classification; 66.08%, 35.09% higher precision for Vascular lesion classification; 42.09%, 65.67% higher precision for Squamous cell carcinoma classification; 32.03%, 43.09% higher precision for seborrheic keratosis classification; 34.65%, 25.88% higher precision for nevus classification evaluated to the existing methods such as SCC-CNN-Squeeze Net-BES and SCD-CNN-GWO respectively.

Table 3: Comparison Of Recall Analysis

Techniques	Recall (%)								
	Melanoma	Basal cell carcinoma	Actinic Keratosis	Pigmented Benign keratosis	Dermatofibroma	Vascular lesion	Squamous cell carcinoma	Seborrheic keratosis	Nevus
SCC-CNN-Squeeze Net-BES	0.77	0.85	0.90	0.86	0.90	0.87	0.77	0.85	0.82
SCD-CNN-GWO	0.82	0.84	0.86	0.75	0.89	0.85	0.89	0.84	0.81
BSNN-GPCOA-AMC-DI(proposed)	0.99	0.98	0.99	1	0.99	0.98	1	0.98	0.99

Table 3 demonstrates the Comparison of Recall analysis. Here, the proposed BSNN-GPCOA-AMC-DI method provides 52.21%, 47.56% higher Recall Melanoma classification; 55.45%, 65.89% higher Recall for Basal cell carcinoma classification; 43.21%, 22.56% higher Recall for Actinic Keratosis classification; 62.45%, 53.89% higher Recall for Benign keratosis classification; 53.98%, 63.44% higher Recall for Dermatofibroma classification; 66.08%, 35.09% higher Recall for Vascular lesion classification; 42.09%, 65.67% higher Recall for Squamous cell carcinoma classification; 43.08%, 22.33% higher recall for seborrheic keratosis classification; 33.22%, 54.44% higher recall for nevus classification evaluated to the existing methods such as SCC-CNN-Squeeze Net-BES and SCD-CNN-GWO respectively.

Table 4: Comparison of F Score Analysis

Techniques	F score (%)								
	Melanoma	Basal cell carcinoma	Actinic Keratosis	Pigmented Benign keratosis	Dermatofibroma	Vascular lesion	Squamous cell carcinoma	Seborrheic keratosis	Neuvs
SCC-CNN-Squeeze Net-BES	0.79	0.85	0.90	0.86	0.90	0.79	0.92	0.87	0.82
SCD-CNN-GWO	0.82	0.84	0.86	0.75	0.89	0.85	0.90	0.85	0.81
BSNN-GPCOA-AMC-DI (proposed)	0.99	0.98	1	0.99	1	0.94	1	0.99	0.99

Table 4 demonstrates the Comparison of F score analysis. Here, the proposed BSNN-GPCOA-AMC-DI method provides 52.21%, 47.56% higher F score for Melanocytic nevus classification; 55.45%, 65.89% higher F score for Basal cell carcinoma classification; 43.21%, 22.56% higher F score for Actinic Keratosis classification; 62.45%, 53.89% higher F score for Pigmented Benign keratosis classification; 53.98%, 63.44% higher F score for Dermatofibroma classification; 66.08%, 35.09% higher F score for Vascular lesion classification; 42.09%, 65.67% higher F score for Squamous cell carcinoma classification; 32.04%, 34.55% higher F score for seborrheic keratosis classification; 12.03%, 11.22% higher F score for nevus classification evaluated to the existing methods such as SCC-CNN-Squeeze Net-BES and SCD-CNN-GWO respectively.

Table 5: Comparison of Sensitivity Analysis

Techniques	Sensitivity (%)								
	Melanoma	Basal cell carcinoma	Actinic Keratosis	Pigmented Benign keratosis	Dermatofibroma	Vascular lesion	Squamous cell carcinoma	Seborrheic keratosis	Neuvs
SCC-CNN-Squeeze Net-BES	0.84	0.87	0.82	0.87	0.82	0.87	0.79	0.88	0.86
SCD-CNN-GWO	0.87	0.85	0.81	0.86	0.87	0.89	0.84	0.87	0.87
BSNN-GPCOA	0.975	0.98	0.97	0.977	0.96	0.984	0.974	0.966	0.98

-AMC-DI(prop osed)									
-----------------------	--	--	--	--	--	--	--	--	--

Table 5 demonstrates the Comparison of sensitivity analysis. Here, the proposed BSNN-GPCOA-AMC-DI method provides 42.21%, 47.56% higher sensitivity for Melanoma classification; 55.45%, 65.89% higher sensitivity for Basal cell carcinoma classification; 43.21%, 22.56% higher sensitivity for Actinic Keratosis classification; 62.45%, 53.89% higher sensitivity for Pigmented Benign keratosis classification; 53.98%, 63.44% higher sensitivity for Dermatofibroma classification; 66.08%, 35.09% higher sensitivity for Vascular lesion classification; 42.09%, 65.67% higher sensitivity for Squamous cell carcinoma classification; 32.03%, 43.09% higher sensitivity for seborrheic keratosis classification; 34.65%, 25.88% higher sensitivity for nevus classification evaluated to the existing methods such as SCC-CNN-Squeeze Net-BES and SCD-CNN-GWO respectively.

Table 5: Comparison of Specificity Analysis

Techniques	Specificity (%)								
	Melanoma	Basal cell carcinoma	Actinic Keratosis	Pigmented Benign keratosis	Dermatofibroma	Vascular lesion	Squamous cell carcinoma	Seborrheic keratosis	Nevus
SCC-CNN-Squeeze Net-BES	0.90	0.89	0.87	0.85	0.83	0.85	0.87	0.87	0.90
SCD-CNN-GWO	0.92	0.88	0.86	0.84	0.82	0.84	0.86	0.88	0.92
BSNN-GPCOA-AMC-DI(prop osed)	0.974	0.984	0.98	0.988	0.986	0.984	0.978	0.975	0.984

Table 5 demonstrates the Comparison of specificity analysis. Here, the proposed BSNN-GPCOA-AMC-DI method provides 42.21%, 47.56% higher specificity for Melanoma classification; 55.45%, 65.89% higher specificity for Basal cell carcinoma classification; 43.21%, 22.56% higher specificity for Actinic Keratosis classification; 62.45%, 53.89% higher specificity for Pigmented Benign keratosis classification; 53.98%, 63.44% higher specificity for Dermatofibroma classification; 66.08%, 35.09% higher specificity for Vascular lesion classification; 42.09%, 65.67% higher specificity for Squamous cell carcinoma classification; 32.03%, 43.09% higher specificity for seborrheic keratosis classification; 34.65%, 25.88% higher specificity for nevus classification evaluated to the

existing methods such as SCC-CNN-Squeeze Net-BES and SCD-CNN-GWO respectively.

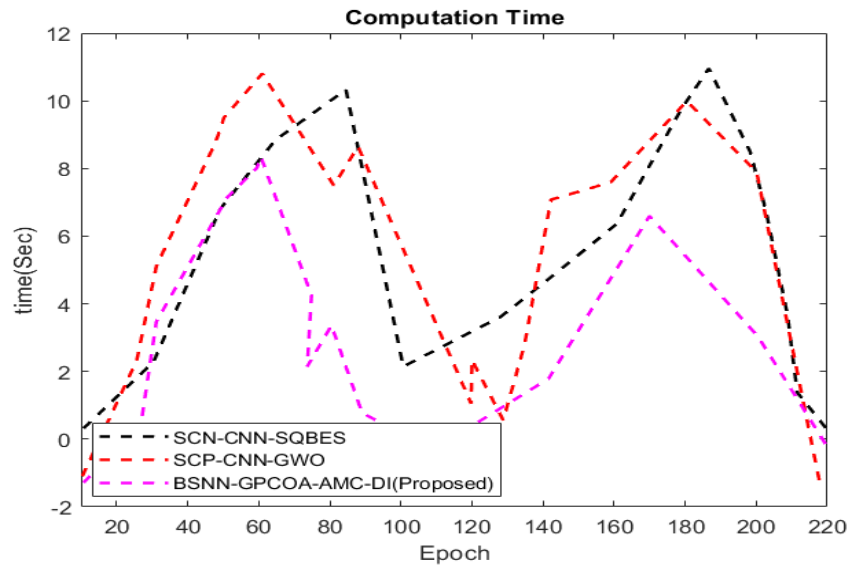


Figure 3: Analysis of Computational Time

Figure 3 shows Computational Time analysis. Here, the proposed BSNN-GPCOA-AMC-DI method provides 32.21%, 37.56% lesser Computation Time evaluated to the existing methods such as SCC-CNN-Squeeze Net-BES and SCD-CNN-GWO respectively.

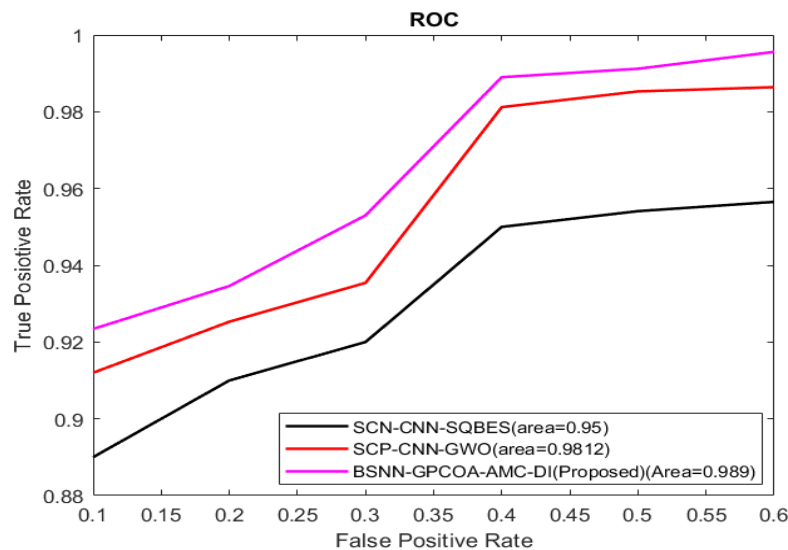


Figure 4: Analysis of Roc

Figure 4 shows ROC analysis. Here, proposed BSNN-GPCOA-AMC-DI method attains 1.01%, 1.02% higher AUC comparing to the existing SCC-CNN-Squeeze Net-BES and SCD-CNN-GWO methods respectively.

4. CONCLUSION

In this section, skin cancer classification using Binarized Spiking Neural Networks optimized with Giza Pyramids Construction Optimization Algorithm was successfully implemented for classifying the skin cancer (BSNN-GPCOA-AMC-DI). The proposed BSNN-GPCOA-AMC-DI approach is implemented in MATLAB utilizing the dataset of skin lesion image. The performance of the proposed BSNN-GPCOA-AMC-DI approach attains 12.015%, 14.928% lower computational time comparing with existing SCC-CNN-Squeeze Net-BES and SCD-CNN-GWO methods.

References

1. Nahata, H. and Singh, S.P., 2020. Deep learning solutions for skin cancer detection and diagnosis. In *Machine Learning with Health Care Perspective* (pp. 159-182). Springer, Cham.
2. Tan, T.Y., Zhang, L. and Lim, C.P., 2020. Adaptive melanoma diagnosis using evolving clustering, ensemble and deep neural networks. *Knowledge-Based Systems*, 187, p.104807.
3. Nawaz, M., Mehmood, Z., Nazir, T., Naqvi, R.A., Rehman, A., Iqbal, M. and Saba, T., 2022. Skin cancer detection from dermoscopic images using deep learning and fuzzy k-means clustering. *Microscopy Research and Technique*, 85(1), pp.339-351.
4. Lafraxo, S., Ansari, M.E. and Charfi, S., 2022. MelaNet: an effective deep learning framework for melanoma detection using dermoscopic images. *Multimedia Tools and Applications*, 81(11), pp.16021-16045.
5. Wei, L., Ding, K. and Hu, H., 2020. Automatic skin cancer detection in dermoscopy images based on ensemble lightweight deep learning network. *IEEE Access*, 8, pp.99633-99647.
6. Sayed, G.I., Soliman, M.M. and Hassanien, A.E., 2021. A novel melanoma prediction model for imbalanced data using optimized SqueezeNet by bald eagle search optimization. *Computers in Biology and Medicine*, 136, p.104712.
7. Mohakud, R. and Dash, R., 2021. Designing a grey wolf optimization based hyper-parameter optimized convolutional neural network classifier for skin cancer detection. *Journal of King Saud University-Computer and Information Sciences*.
8. Kumar, M., Alshehri, M., AlGhamdi, R., Sharma, P. and Deep, V., 2020. A de-ann inspired skin cancer detection approach using fuzzy c-means clustering. *Mobile Networks and Applications*, 25, pp.1319-1329.
9. Balaji, M., Saravanan, S., Chandrasekar, M., Rajkumar, G. and Kamalraj, S., 2021. Analysis of basic neural network types for automated skin cancer classification using Firefly optimization method. *Journal of Ambient Intelligence and Humanized Computing*, 12(7), pp.7181-7194.
10. Kumar, M.P., Poornima, B., Nagendraswamy, H.S. and Manjunath, C., 2021. Structure-preserving NPR framework for image abstraction and stylization. *The Journal of Supercomputing*, 77(8), pp.8445-8513.
11. Wang, L., Wang, H., Han, X. and Zhou, W., 2021. A novel adaptive density-based spatial clustering of application with noise based on bird swarm optimization algorithm. *Computer Communications*, 174, pp.205-214.
12. Tuncer, T., Dogan, S. and Subasi, A., 2020. Surface EMG signal classification using ternary pattern and discrete wavelet transform based feature extraction for hand movement recognition. *Biomedical signal processing and control*, 58, p.101872.

13. Kheradpisheh, S.R., Mirsadeghi, M. and Masquelier, T., 2022. Bs4nn: Binarized spiking neural networks with temporal coding and learning. *Neural Processing Letters*, 54(2), pp.1255-1273.
14. Harifi, S., Mohammadzadeh, J., Khalilian, M. and Ebrahimnejad, S., 2021. Giza Pyramids Construction: an ancient-inspired metaheuristic algorithm for optimization. *Evolutionary Intelligence*, 14(4), pp.1743-1761.
15. <https://www.kaggle.com/datasets/andrewmvd/isic-2019>